APP Template V1.00 Article id: mrxaa1876 Typesetter: MPS Date received by MPS: 24/02/2016 PE: MAC003305 CE: LE: UNCORRECTED PROOF

IOP Publishing *Mater. Res. Express* **00** (2016) 000000

Materials Research Express

RECEIVED
2 December 2015

REVISED
4 February 2016

ACCEPTED FOR PUBLICATION
18 February 2016

PUBLISHED
DD MM 2016

PAPER

Limitations of high pressure sputtering for amorphous silicon deposition

R García-Hernansanz[1,2], E García-Hemme[1,2], D Montero[1,2], J Olea[1,2], E San Andrés[1,2], A del Prado[1,2], F J Ferrer[3], I Mártil[1,2] and G González-Díaz[1,2]

[1] Dpto. Física Aplicada III, Universidad Complutense de Madrid. Spain
[2] CEI Campus Moncloa, UCM-UPM, 28040 Madrid, Spain
[3] Centro Nacional de Aceleradores, Universidad de Sevilla-CSIC, Spain

E-mail: rodgar01@ucm.es

Keywords: high pressure sputtering, hydrogenated amorphous silicon, high deposition rate

Abstract

Amorphous silicon thin films were deposited using the high pressure sputtering (HPS) technique to study the influence of deposition parameters on film composition, presence of impurities, atomic bonding characteristics and optical properties. An optical emission spectroscopy (OES) system has been used to identify the different species present in the plasma in order to obtain appropriate conditions to deposit high purity films. Composition measurements in agreement with the OES information showed impurities which critically depend on the deposition rate and on the gas pressure. We prove that films deposited at the highest RF power and 3.4×10^{-2} mbar, exhibit properties as good as the ones of the films deposited by other more standard techniques.

1. Introduction

Hydrogenated amorphous silicon (a-Si:H) has been thoroughly studied in the last decades. Its excellent electro optical properties have made it a key choice to be used in optoelectronic devices [1, 2]. Usually, a-Si:H is deposited by chemical vapor deposition (CVD), however, sputter deposition could be an interesting alternative in order to increase the scalability and to avoid the use of SiH_4 and other hazardous gases. This technique allows the deposition of a-Si:H films using inert gases (such as argon) at low temperatures, with high reproducibility.

In conventional sputtering systems (RF, magnetron), the gas pressure during deposition is normally comprised in the range of 10^{-2}–10^{-3} mbar [3, 4]. For a typical sputtering pressure of 5×10^{-3} mbar the mean free path of electrons is around 110 mm and the mean free path of ions and neutrals is around 1 mm [5]. Thus, the substrate surface can be damaged by bombardment of negatively ionized species or by electrons. This may lead to a film re-sputtering and, consequently, to the generation of defects at the a-Si:H/Substrate interface.

To prevent this effect, in this work we have used a non-conventional High Pressure Sputtering (HPS) system to deposit the a-Si:H films. The working pressure of our system can be varied from 10^{-2} mbar to 5 mbar so that the mean free path of the plasma species is greatly reduced. For instance, at a working pressure of 1 mbar, the particles emitted by the target collide with the gaseous medium, losing its energy and thermalizing within a short distance of the cathode (around 2 mm for sputtered atoms and 3 mm for reflected atoms) [6] and then reach the substrate by a pure diffusion process. At this pressure, the mean free path for electrons is about 0.5 mm and only of about 0.05 mm for ions [7]. Therefore, the HPS deposition method prevents the impact of high-energy species on the substrate, greatly reducing the damage to the interface and to the growing film.

Seminal papers dealing with the HPS technique have proven the feasibility of this technique to successfully grow high-Tc superconductor films [8] and multilayer buffers for high-Tc superconductor devices [9]. More recently, HPS has been used to deposit high permittivity dielectrics such as HfO_2 and Gd_2O_3 [10–12]. However, high pressure plasmas are known to be a propitious environment for the formation of dust particles [13] that could be related with the presence of undesirable species in the plasma.

© 2016 IOP Publishing Ltd

The aim of this paper is to analyze the main characteristics of the deposition of a-Si:H films in HPS systems, with emphasis in the advantages and drawbacks inherent to this deposition technique. We will face the problem of impurities in HPS systems and discuss some possible ways to solve it.

2. Experimental details

The HPS system used in this work consists of a cylindrical chamber evacuated with a turbomolecular-mechanical pumping set. During plasma processes, we adjust the pumping speed using a manual high vacuum throttle valve. The cathode assembly was manufactured at the Center of Nanoelectronic Systems for Information Technology (Germany) and is specifically designed for HPS systems. The target is a disk of single-crystalline silicon, 3 mm thick and 50 mm diameter with 99.999% purity, supplied by Kurt Lesker and it is epoxy bonded to a Cu disk screwed to the cathode assembly. In our system, the target-substrate distance, the substrate temperature and the working pressure can be adjusted.

The plasma is excited by a Hüttinger PFG 300 RF power supply working at a frequency of 13.56 MHz. The incident RF power used in this work ranged from 40 W to 110 W and in order to avoid thermal stressing of the target, we raised the RF power at a slow rate of 0.2 W s^{-1}. The impedance of the RF supply is matched to the plasma impedance by a matching network and no reflected power was detected at any deposition condition.

The base pressure was typically 5×10^{-7} mbar and for film deposition processes we introduced high purity argon (99.9999%) and hydrogen (99.999%). The pressure during deposition was varied from 10^{-2} to 1 mbar. The plasma light emission was monitored using four Stellarnet miniature spectrometers coupled to a quartz window on the sputtering chamber through optical fibers. The spectrometers cover the range from 200 nm to 1000 nm and have a resolution of 0,25 nm. Optical emission spectroscopy (OES) in real time is an essential tool to determine the presence of impurities in the gas, target impurities and vacuum leaks.

Films between 100 to 500 nm have been deposited on two kinds of substrates: quartz, intended for optical characterization, and crystalline silicon (both sides polished, $\rho > 10.000$ Ωcm, d = 500 μm) intended for compositional measurements.

In order to study the bonding structure of the films, FTIR (Fourier Transform Infrared) spectroscopy measurements has been conducted with a Nicolet Magna-IR 752 spectrometer, operated in transmission mode at normal incidence, at wavenumbers ranging from 340 cm^{-1} to 4000 cm^{-1}.

We have used Rutherford Backscattering Spectrometry (RBS) to determine the Si concentration, Elastic Recoil Detection Analysis (ERDA) for H concentration, and Nuclear Reaction Analysis (NRA) for possible contaminants like N, C and O. From these techniques, we have obtained the atomic concentration of each one of these elements.

For RBS measurements, we used an alpha particle beam of 1.0 MeV. A 7° tilt has been given to the samples and and a detector placed at 165° collected the scattered particles. To determine the concentration of N in the samples, we used the nuclear reaction 15N (d, α)13C with deuterons with energy of 1.4 MeV and the detector placed at 150° as compilation angle. In order to stop the backscattered deuteron ions, a 13 μm aluminized Mylar foil was used as an absorber. To obtain the O concentration, we used the $^{16}O(d,p)^{17}O$ nuclear reaction with deuterons with energy of 1.15 MeV, in the same set-up. ERDA measurements were performed using He^{2+} ions with energy of 3.0 MeV. The dispersion angle was 34°, and a collimator was placed in front of the detector to pick-up only particles with this angle. To avoid the arrival of scattered He^{2+} ions to the detector, we placed a 13 μm thickness absorber of aluminized Mylar also in front of the detector.

The optical properties of the deposited a-Si:H films were obtained by means of transmittance and reflectance measurements in a Perkin Elmer Lambda 1050 UV/Vis/NIR spectrophotometer, in the 300 nm–1700 nm wavelength range. From the spectra, the optical band-gap was determined following the well-known Tauc relation [14].

3. Results and discussion

Figure 1 presents the OES spectra of a plasma working at 1 mbar pressure and at two different values of RF power: 40 W and at 90 W in pure Ar, i.e. without H. The most intense line at 294 nm corresponds to argon, but the most important information is obtained from the lines at 251.5 nm and 288.1 nm that belong to silicon emissions [15] and from the set of peaks at around 336 nm. For clarity, we present a magnification of this group in figure 1(b). We must take into account that the observed intensity in the OES spectra depends on the emission intensity of each element or molecule. Therefore, each band in the OES spectra can only be compared with the same band. The emission line at 336 nm is the well-known persistent line $A^3\Pi$—$X^3\Sigma^-$ of NH [15]. This peak is very dependent on the vacuum conditions and also on the target and chamber cleaning procedure. We observe a decrease of the NH intensity line to a final limit which is slightly dependent on the RF power. The ratio between

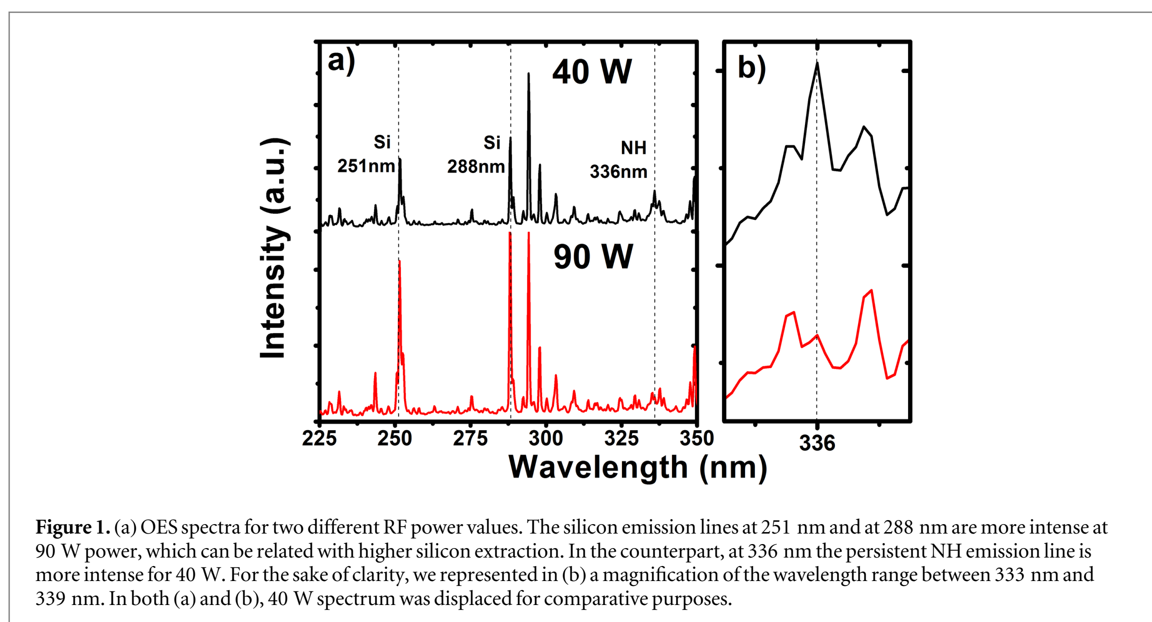

Figure 1. (a) OES spectra for two different RF power values. The silicon emission lines at 251 nm and at 288 nm are more intense at 90 W power, which can be related with higher silicon extraction. In the counterpart, at 336 nm the persistent NH emission line is more intense for 40 W. For the sake of clarity, we represented in (b) a magnification of the wavelength range between 333 nm and 339 nm. In both (a) and (b), 40 W spectrum was displaced for comparative purposes.

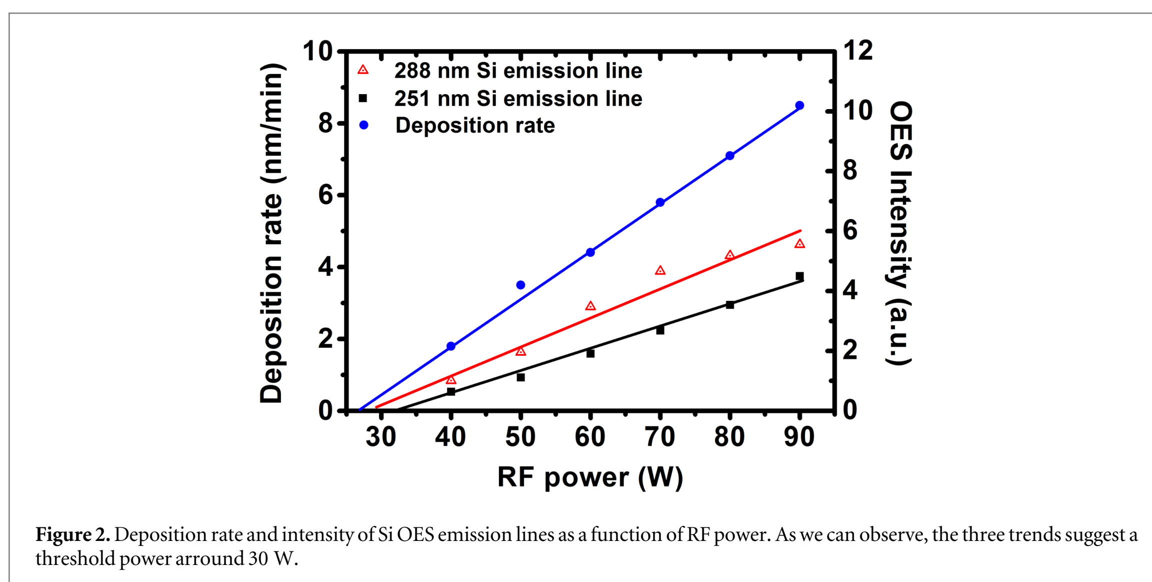

Figure 2. Deposition rate and intensity of Si OES emission lines as a function of RF power. As we can observe, the three trends suggest a threshold power arround 30 W.

the intensities of Si and NH lines increases as the RF power raises from 40 to 90 W pointing to a better purity of the deposited film. Indeed, at 90 W the silicon emission lines become the most intense in the spectra. The N presence in the chamber is remarkable considering the absence of N sources and the low base pressure before starting the process (5×10^{-7} mbar).

In figure 2 we have represented the a-Si:H film deposition rate as a function of the RF power for samples deposited at 1 mbar. A linear trend, which intersects the RF power axis at 30 W is observed. In the same figure, we have also shown the OES intensities of the silicon emission lines at 251.5 nm and 288.1 nm. It is remarkable that these intensities have the same intersection with the RF power axis as the deposition rate. Below 30 W no silicon lines were observed in spite of the fact that the plasma could be ignited at power values as low as 5 W. This threshold value could indicate that below 30 W, the ionized argon atoms do not have enough energy to extract Si atoms from the target. Given the good correlation between the Si emission lines and deposition rate, the intensity of these lines can be used as a real time indication of growth dynamics.

Figure 3 shows the relative concentrations of Si, H, O and N in the films as a function of RF power. For these samples, prior to film deposition we introduced high purity hydrogen (99.999%) in the chamber for 15 min at a pressure of 3×10^{-1} mbar without plasma ignition. This procedure is intended to favor the formation of Si-H bonds in our films by saturation of the chamber walls. After saturating the sputtering chamber walls with H, we stopped the H introduction, we introduced pure Ar (99.9999%) and then, we ignited the plasma and performed a target conditioning process while the substrate holder is covered with a shutter. This conditioning process lasts

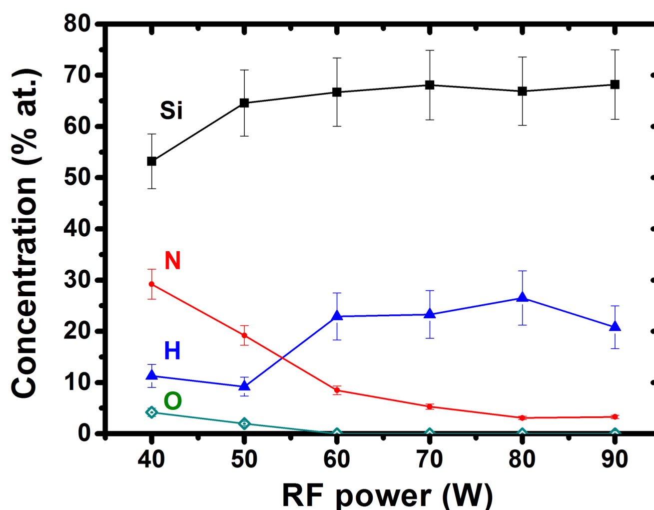

Figure 3. Concentration of Si, H, O and N for films deposited at 1 mbar, at different RF powers values. As we can observe, above 60 W the film has less N and O and more H content.

1 h. Finally, we performed all the sputtering processes in Ar atmosphere at 1 mbar pressure, without introducing H during film deposition.

Note that for the films deposited at 40 W, a 30% of N was incorporated into the film, while the one deposited at 90 W only incorporates a 3%. This is in agreement with the optical spectroscopy presented in figure 1. This nitrogen is undesirable, since silicon rich nitride behaves like an insulator [16]. According to figure 3, we conclude that at RF powers over 60 W, the N incorporation in the film is below 5%, and we obtain better purity a-Si:H films. Figure 3 also suggests a competitive behavior of both N and H in order to be bonded to Si atoms. It seems that, for high RF-powers, the hydrogen present in the chamber bonds with silicon atoms, and results in a high hydrogen concentration in the films. It is noticeable that, even without supplying hydrogen to the plasma atmosphere, the low amount of hydrogen desorbed from the saturated walls is incorporated to the film up to a 25% concentration. Also, in figure 3, we can observe that the Si and H concentration for films deposited at RF power above 60 W remains almost constant. The same behavior is observed for the O and N concentrations when sputtering above 80 W, being the concentration of both elements marginal.

It is important to note the N and O concentration in the films, mainly at low RF power values. The origin of the presence of these elements will be analyzed below. First of all, we discard an air leakage in the system because the base pressure before starting the process is very low (5×10^{-7} mbar). We have calculated the atomic Si, N and O incorporation rates per unit area by dividing the atomic concentrations per unit area (obtained from the composition measurements) by the deposition time. We obtain this atomic flux for the same six samples presented in figure 3. In figure 4 we show the Si and N atomic flux impinging the substrate as a function of RF power. In this picture we do not represent the flux for the oxygen as this rate is much lower than the ones for N and Si. The maximum rate for this element, calculated for the sample grown at 40 W is as low as $Z_{O40W} = 3 \times 10^{12}$ cm^{-2} s^{-1}.

The Si incorporation rate increases linearly when increasing the RF power from $Z_{Si40W} = 3.4 \times 10^{13}$ cm^{-2} s^{-1} at 40 W to $Z_{Si90W} = 5.1 \times 10^{14}$ cm^{-2} s^{-1} at 90 W. As we expected, this linear trend intersects the RF power axis at 30 W, the same threshold value that we have obtained from OES intensities and from the deposition rate.

This result is consistent with the higher intensity of the Si emission lines observed by OES (figure 1), as well as the higher deposition rate obtained at higher RF power, and it is a consequence of an improved efficiency of extraction of Si atoms from the target when RF power is increased. However, the N incorporation rate remains roughly constant at about $Z_N = 2.5 \times 10^{13}$ cm^{-2} s^{-1}, and does not exhibit any dependence on the RF power. Since the incorporation of N is not enhanced by increasing the RF power, we conclude that the origin of the N concentration cannot be related to target contamination. Also, any variation in target composition during deposition causes changes in the impedance of the system. As a result, the capacity of the two capacitors in the matching network should be changed in order to minimize the reflected power to the RF-power supply. However, we never observed any change during film deposition, indicating the homogeneity of the process.

To confirm this result we present in figure 5 the FTIR absorbance spectra normalized to the film thickness for films deposited at 1 mbar and variable RF power values. In the figure we can observe two bands at 647 cm^{-1} and 2090 cm^{-1} corresponding to the Si-H wagging mode [17] and the Si-H_2 stretching mode, respectively, as

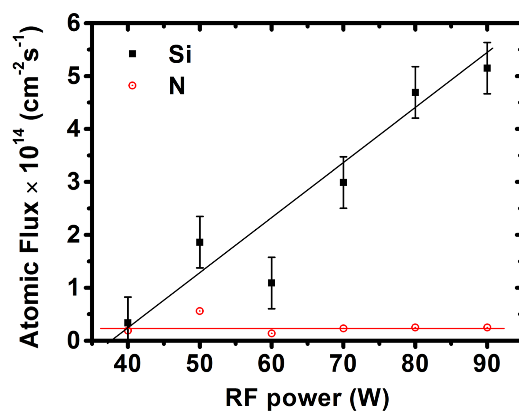

Figure 4. Si and N atomic flux incorporated to the substrate per area unit as a function of RF power. While Si flux increases with the RF power, N flux remains almost constant.

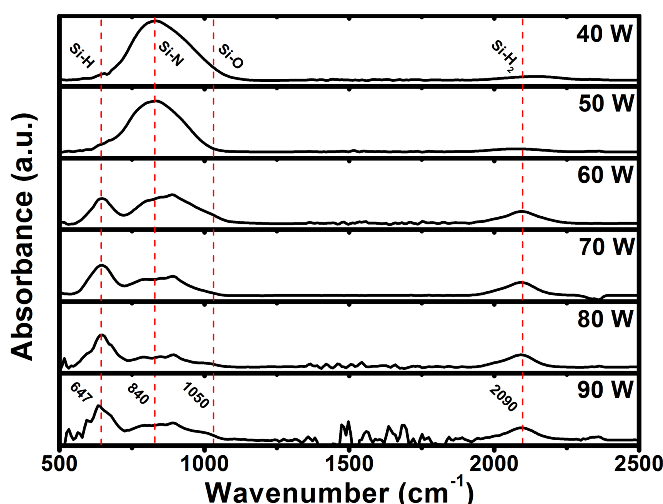

Figure 5. FTIR absorbance spectra normalized to thickness for samples deposited at 1 mbar and different RF power. As we can observe, the Si-N absorption band at 840 cm^{-1} dominates for low RF-power. As the RF-power increases, the Si-H bands at 647 cm^{-1} and 2090 cm^{-1}, are more intense.

well as three different bands around 840 cm^{-1}. These bands correspond to the Si-H bending (802 cm^{-1}), the Si-N stretching (840 cm^{-1}) [18] and the Si-H_2 bending (882 cm^{-2}) modes. At 1050 cm^{-1} it is expected the Si-O related band [19], but for these samples it is almost negligible.

The behavior of all these bands is in full agreement with the results of the composition and OES measurements. As the RF power is increased, the N incorporation on the films becomes lower, as evidenced by the decrease of the absorbance of the Si-N band, reaching its lower limit at 80–90 W.

On the other hand, the absorbance of the bands related to the Si-H bonds clearly increases with RF power up to 60 W, when it remains almost constant. According to these results, the H incorporation does not seem to come from N-H impurities, because the Si-H and Si-N bands show competitive trends. Additionally, no bands related with N-H bonds were observed.

The dependence of the composition of the films with the RF power is explained by the Si extraction improvement. This results in a higher incorporation rate of Si into the film, therefore for high growth rates a-Si:H films are obtained with a residual N content. Also, the incorporation of H as Si-H bonds is enhanced. However, this competitive trend stops at 80 W, when the Si-H/Si-N relation remains constant.

As the HPS system works at a pressure about three orders of magnitude higher than the usual magnetron sputtering systems, the number of gas atoms in the chamber during the plasma process has the same ratio. Consequently, when using Ar with the same purity, the residual contaminating gases during the process will also be three orders of magnitude higher. Since the deposition rate is typically lower for HPS systems, the possibility of impurity incorporation is clearly enhanced.

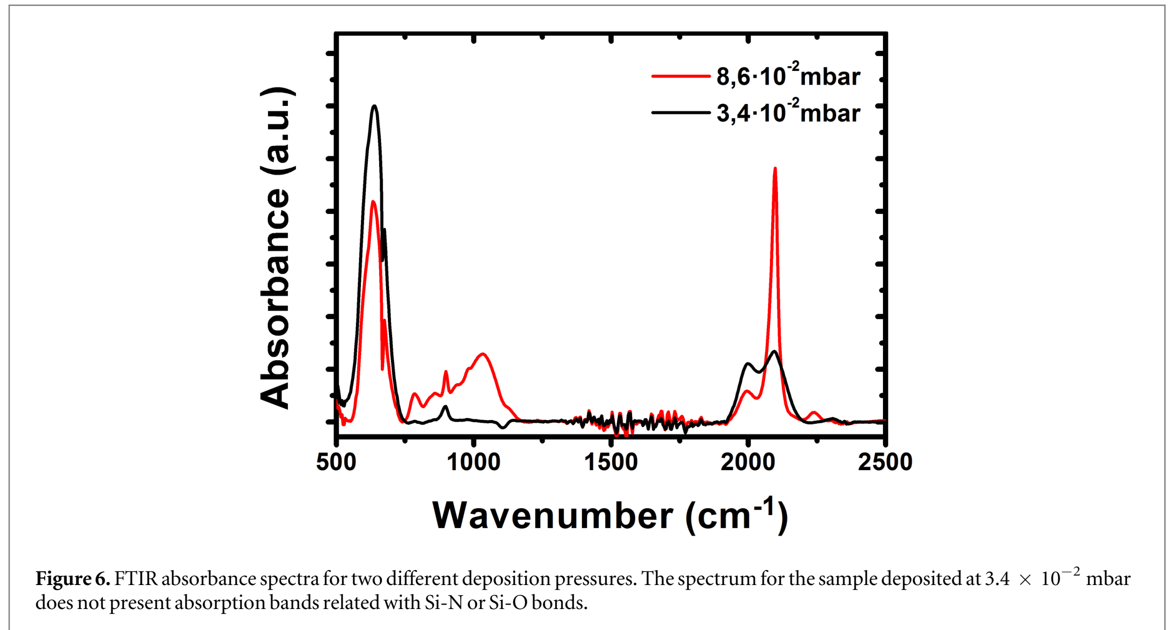

Figure 6. FTIR absorbance spectra for two different deposition pressures. The spectrum for the sample deposited at 3.4×10^{-2} mbar does not present absorption bands related with Si-N or Si-O bonds.

To support this discussion, we will calculate the nitrogen impingement rate, i.e., the number of N particles that reach the substrate per second and unit area. In this point it is important to note that this parameter is different than the atomic flux calculated in figure 4. The atomic flux is obtained from the film composition and it is the true rate of N incorporated. However, the impingement rate is a calculated value that only depends on pressure, temperature and molecular weight as can be observed in equation (1). When working at 1 mbar total pressure with 99.9999% Ar, the N partial pressure, assuming that all the impurities in the Ar cylinder are N, should be 10^{-6} mbar. In that case the impingement rate can be calculated by [20]:

$$z = \frac{n \cdot \bar{v}}{4} \mathrm{cm}^{-2}\,\mathrm{s}^{-1} \tag{1}$$

Where:

$$n = \frac{P}{KT} \qquad \bar{v} = \sqrt{\left(\frac{8KT}{\pi m}\right)}$$

Finaly equation (1) becomes:

$$z = \sqrt{\left(\frac{N_A}{2\pi K}\right)} \cdot \frac{P}{\sqrt{W_m T}} \mathrm{cm}^{-2}\,\mathrm{s}^{-1} \tag{2}$$

In equation (2), W_m is the molecular weight (28 for N_2), N_A is the Avogadro constant, K the Boltzmann constant, P is the N partial pressure (1×10^{-4} Pa), and T is the gas temperature near the sample (400 K) [21]. From equation (2) we obtain an impingement ratio of $z = 2.5 \times 10^{14}$ cm^{-2} s^{-1}. Now, if we divide the atomic flux calculated in figure 4 by this impingement rate, we obtain the sticking coefficient with a value of roughly 10%. This figure is, of course, a crude estimation. If the residual gas in the Ar cylinder was not composed entirely of N, this sticking coefficient would be higher. Anyway the minimum of 10% seems to be a realistic value.

In conclusion, to obtain good quality a-Si:H films on a HPS system, we are limited by the purity of the process gas, and in the case of 99.9999% Ar purity it is advisable to work at pressures under 1 mbar.

From equation (1), to reduce the rate of impurities impingement, we need to rise the process temperature and/or decrease the deposition pressure, but the most relevant parameter is the last one. In figure 6 we show the FTIR spectra of two samples deposited at 400 °C, 110 W and two different pressures: 8.6×10^{-2} mbar and 3.4×10^{-2} mbar. We can observe that the sample deposited at 3.4×10^{-2} mbar does not exhibit any absorption band related with N (840 cm^{-1}) or O (1050 cm^{-1}), thus confirming the previous discussion, i.e., lowering the deposition pressure substantially avoids the contamination problem which was analyzed in this paper. Also, the deposition rate increases considerably up to a value of 17 nm min^{-1} for the sample fabricated at the lowest pressure.

For the sample deposited at 8.6×10^{-2} mbar, the Si-O absorption band located at ~1050 cm^{-1} is now observed because it is not masked by the Si-N absorption band at 840 cm^{-1} that does not appear in any of the spectra.

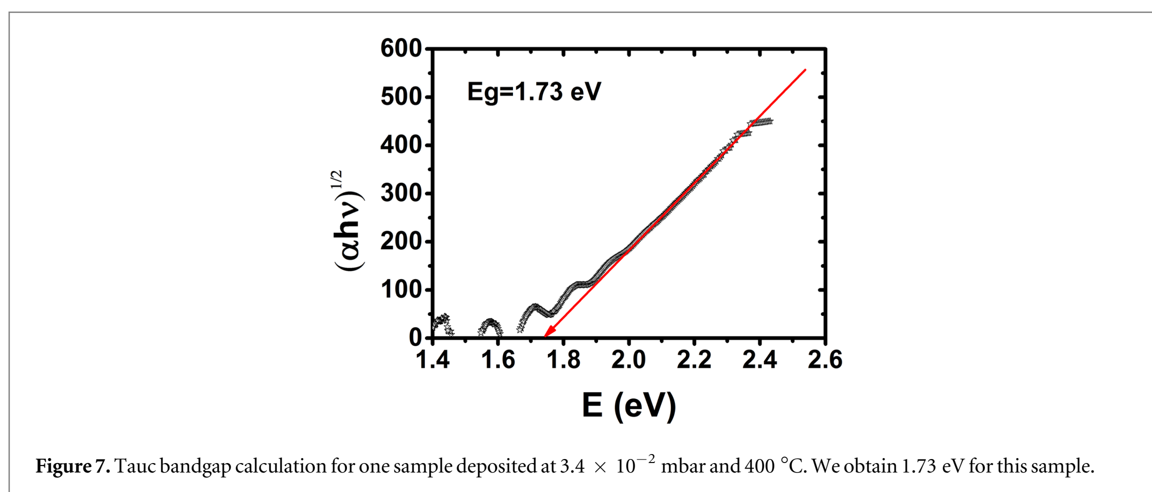

Figure 7. Tauc bandgap calculation for one sample deposited at 3.4×10^{-2} mbar and 400 °C. We obtain 1.73 eV for this sample.

In relation with the Si-H bands, on samples deposited at 1 mbar in figure 5 we only observed two bands related with silicon and hydrogen, one at 647 cm^{-1} corresponding to the Si-H wagging mode and the other at 2090 cm^{-1} corresponding to the Si-H_2 stretching mode. However, in figure 6, we can clearly observe the Si-H stretching mode at 2000 cm^{-1}. This band is related with good passivation of c-Si wafers with a-Si:H, because, as it is well known, when the dominant bonds are Si-H_2, a higher the density of microvoids and defects is present in the film, thus reducing the film quality [22].

To make a full characterization of our a-Si:H films, we have also obtained the optical band gap of the films [23]. For samples deposited at 1 mbar and 80 W, we obtain band gap values in the range of 2.15 eV, that is higher than the referenced value for a-Si:H, but is the one expected for a-Si:H with N content [24]. However, as we can observe in figure 7, for samples deposited at 3.4×10^{-2} mbar and 400 °C the Tauc bandgap value is 1.73 eV as expected for high quality a-Si:H [25]. These values support our discussion concerning N incorporation in the films when working in the mbar range.

According to the previous results, it is clear that a pressure interval for optimum film production in a HPS equipment exists. High pressures produce low film damage while low pressures minimize the incorporation of impurities (N and O) in the film. In our case the optimum pressure is about 3.4×10^{-2} mbar.

4. Summary and conclussions

In this work, we have deposited a-Si:H layers using HPS. We have found that the main contaminating element in the film is N, coming from the process gas, in spite of its high purity (99.9999% Ar in our case). To avoid the presence of N or other contaminants in the growing film it is advisable to obtain the maximum deposition velocity, which in turn is obtained with the maximum Si extraction rate. For this purpose we need to increase the RF power and to diminish the pressure. This implies a process window in the pressure since high pressures produce low damage to the growing films, but, as it was proven in this work, also higher contamination. In our case, since the rf power was limited to 110 W by target refrigeration issues, the maximum pressure with good a-Si:H properties was 3.4×10^{-2} mbar. At these deposition conditions films with a band gap of 1.73 eV and a FTIR spectrum with just Si-H bonds are obtained, indicating a high purity film composition.

In conclusion, we have shown that the HPS deposition technique can be a valuable procedure to deposit a-Si:H when we can work in the high deposition rate regime.

Acknowledgement

Authors would like to acknowledge the CAI de Técnicas Físicas and C.A.I de Espectroscopía of the Universidad Complutense de Madrid for the use of its laboratories and FTIR measurements. This work was partially supported by the Project MADRID-PV (Grant No. 2013/MAE-2780) funded by the Comunidad de Madrid, by the Spanish MINECO (Ministerio de economía y competitividad) under grant TEC 2013-41730-R and by the Universidad Complutense de Madrid (Programa de Financiación de Grupos de Investigación UCM–Banco Santander) under grant 910173-2014. D. Montero acknowledges the Spanish MINECO (Ministerio de economía y competitividad) for financial support under contract BES-2014-067585

Q1

References

[1] Zhang R, Chen X Y, Zhang K and Shen W Z 2006 *J. Appl. Phys.* **100** 104310

[2] Tsunomura Y, Yoshimine Y, Taguchi M, Baba T, Kinoshita T, Kanno H, Sakata H and Tanaka M 2009 *Sol. Energy Mater. Sol. Cell* **93** 670

[3] Kim D Y, Kim I S and Choi S Y 2009 *Sol. Energy Mater. Sol. Cell* **93** 239

[4] Jagannathan B, Anderson W A and Coleman J 1997 *Sol. Energy Mater. Sol. Cell* **46** 289

[5] Chapman B 1980 *Glow Discharge Processes* (New-York NY: J. Wiley)

[6] Toledano-Luque M, San Andrés E, del Prado A, Mártil I, González-Díaz G, Martínez F L, Bohne W, Röhrich J and Strub E 2007 *J. Appl. Phys.* **102** 044106

[7] Westwood W and Mattox D 1977 *Sputtering* (New-York NY: AVS)

[8] Poppe U, Schubert J, Arons R R and Evers W Freiburg C, Reichert W, Schmidt K, Sybertz W and Urban K 1988 *Solid State Commun.* **66** [illegible]

[9] Fa[illegible]I, Mi S B, Petraru A, Jia C L, Poppe U and Urban K 2006 *Appl. Phys. Lett.* **89** 082507

[10] Feijoo P C, Pampillón M A and San Andrés E 2015 *Thin Solid Films* **593** 62

[11] Pampillón M A, Feijoo P C, San Andrés E, García H, Castán H and Dueñas S 2015 *Semicond. Sci. Technol.* **30** 035023

[12] Pampillón M A, Cañadilla C, Feijoo P C, San Andrés E and del Prado A 2013 *J. Vac. Sci. Technol.* B **31** 01A1[illegible]

[13] Nafarizal N and Sasaki K 2012 *J. Phys. D: Appl. Phys.* **45** 505202

[14] Hernandez-Rojas J L, Lucía M L, Mártil I, González-Díaz G, Santamaría J and Sánchez-Quesada F 1992 *Appl. Optics* **31** 1606

[15] Pearse R W B and Gaydon A G 1976 *The identification of Molecular Spectra* (London: Chapman and Hall)

[16] Martínez F L, San Andrés E, del Prado A, Mártil I, Bravo D and López F J 2001 *J. Appl. Phys.* **90** 3

[17] Mahan A H, Gedvilas L M and Webb J D 2000 *J. Appl. Phys.* **87** 1650

[18] Rong-Hwei Y, Tai-Rong Y, Te-Cheng C, Shih-Yung L and Jyh-Wong H 2008 *IEEE Trans. Electron Devices* **55** 978

[19] Kilper T *et al* 2009 *J. Appl. Phys.* **105** 074509

Q2 [20] Umrath W 1998 *Fundamentals of Vacuum Tech[illegible]*

Q3 [21] Bogaerts A, Gijbels R and Serikov V 2000 *J. Appl*[illegible]

[22] Meddeb H, Bearda T, Abdelraheem Y, Ezzaouia H, [illegible]on1 I, Szlufcik J and Poortmans J 2015 *J. Phys. D: Appl. Phys.* **48** 415301

[23] Tauc J, Grigorov R and Vancu A 1966 *Phys. Status Solidi* **15** 627

[24] Giorgis F, Pirri C F, Tresso E, Rigato V, Zandolin S and Rava P 1997 *Physica* B **229** 233

[25] Cody G D, Brooks B G and Abeles B 1982 *Sol. Energy Mater.* **8** 231

QUERY FORM

JOURNAL: Materials Research Express

AUTHOR: R García-Hernansanz *et al*

TITLE: Limitations of high pressure sputtering for amorphous silicon deposition

ARTICLE ID: mrxaa1876

The layout of this article has not yet been finalized. Therefore this proof may contain columns that are not fully balanced/matched or overlapping text in inline equations; these issues will be resolved once the final corrections have been incorporated.

We have been provided funding information for this article as below. Please confirm whether this information is correct. Universidad Complutense de Madrid: 910173-2014; Comunidad de Madrid: 2013/MAE-2780; Ministerio de Economía y Competitividad: BES-2014-067585, TEC 2013-41730-R.

Page 8

Q1
Please check the details for any journal references that do not have a link as they may contain some incorrect information.

Page 8

Q2
Please provide the volume and page number or article number in reference [20].

Page 8

Q3
Please provide the page range or article number in reference [21].